4th Hinode *Science Meeting: Unsolved Problems and Recent Insights*
ASP Conference Series, Vol. 455
L. R. Bellot Rubio, F. Reale, and M. Carlsson, eds.
©2012 Astronomical Society of the Pacific

First Results from the SUNRISE Mission

S. K. Solanki,[1,8] P. Barthol,[1] S. Danilovic,[1] A. Feller,[1] A. Gandorfer,[1] J. Hirzberger,[1] S. Jafarzadeh,[1] A. Lagg,[1] T. L. Riethmüller,[1] M. Schüssler,[1] T. Wiegelmann,[1] J. A. Bonet, [2] M. J. Martínez González,[2] V. Martínez Pillet,[2] E. Khomenko,[2] L. Yelles Chaouche,[2] J. C. del Toro Iniesta,[3] V. Domingo,[4] J. Palacios,[4] M. Knölker,[5] N. Bello González,[6] J. M. Borrero,[6] T. Berkefeld,[6] M. Franz,[6] M. Roth,[6] W. Schmidt,[6] O. Steiner,[6] and A. M. Title[7]

[1]*Max-Planck-Institut für Sonnensystemforschung, Max-Planck-Str. 2, 37191 Katlenburg-Lindau, Germany; email: solanki@mps.mpg.de*

[2]*Instituto de Astrofísica de Canarias, C/Vía Láctea s/n, 38200 La Laguna, Tenerife, Spain.*

[3]*Instituto de Astrofísica de Andalucía (CSIC), Apdo. de Correos 3004, 18080, Granada, Spain*

[4]*Grupo de Astronomía y Ciencias del Espacio (Univ. de Valencia), E-46980, Paterna, Valencia, Spain*

[5]*High Altitude Observatory, National Center for Atmospheric Research, P.O. Box 3000, Boulder CO 80307-3000, USA.*

[6]*Kiepenheuer-Institut für Sonnenphysik, Schöneckstr. 6, 79104 Freiburg, Germany.*

[7]*Lockheed-Martin Solar and Astrophysics Lab., Palo Alto, USA*

[8]*School of Space Research, Kyung Hee University, Yongin, Gyeonggi, 446-701, Korea*

Abstract. The SUNRISE balloon-borne solar observatory consists of a 1m aperture Gregory telescope, a UV filter imager, an imaging vector polarimeter, an image stabilization system, and further infrastructure. The first science flight of SUNRISE yielded high-quality data that reveal the structure, dynamics, and evolution of solar convection, oscillations, and magnetic fields at a resolution of around 100 km in the quiet Sun. Here we describe very briefly the mission and the first results obtained from the SUNRISE data, which include a number of discoveries.

1. Introduction

SUNRISE is the latest in a long line of solar telescopes carried by stratospheric balloons. It combines high spatial resolution with sensitivity to ultraviolet radiation. At 1 m diameter, it is the largest solar telescope to leave the ground as of now. It is equipped

with state-of-the-art post-focus instruments, including a UV imager and a filter-based vector magnetograph.

The magnetic field in the solar photosphere shows a very complex and diverse structure. Concentrations of magnetic field with kilo-Gauss strength appear in a broad range of sizes reaching down to small flux concentrations on scales of 100 km or below. SUNRISE aims to determine the true size and brightness distribution of the concentrated magnetic features by spatially resolving them, as well as providing greatly improved properties of the internetwork fields. SUNRISE also aims to probe the convection in the solar photosphere, as well as the often complex effects of the interaction of the magnetic field with the turbulent convection.

SUNRISE can be seen to complement the Solar Optical Telescope (Tsuneta et al. 2008) on *Hinode* (Kosugi et al. 2007) in a number of ways. *Hinode* boasts an excellent spectropolarimeter, has been following the Sun uninterruptedly for a number of years, provides longer time series, in particular in visible bands, and allows a better comparison with transition region and coronal data, while SUNRISE achieves a higher spatial resolution (critical for the study of small-scale magnetic features), covers the poorly studied near UV, and obtains excellent high-cadence magnetograms at multiple wavelengths within a high-Landé factor line.

2. Instrumentation and Mission

The SUNRISE stratospheric balloon-borne observatory is composed of a telescope, two post-focus science instruments (called SuFI and IMaX, see below), an Image Stabilization and Light Distribution (ISLiD) unit, and a Correlating Wave-front Sensor (CWS), all supported by a protective gondola, which possesses pointing capability.

The telescope is a Gregory-type reflector with 1 m clear aperture and an effective focal length of close to 25 m. A heat-rejection wedge at the prime focus reflects 99% of the light from the solar disk off to the side, reducing the heat load on the post-focus instruments to approximately 10 W. The secondary mirror is actively controlled in three degrees of freedom to compensate for thermoelastic deformations of the telescope during flight. The post-focus instrumentation rests on top of the telescope. More details on the telescope, gondola and mission are given by Barthol et al. (2011). The SUNRISE Filter Imager (SuFI; see Gandorfer et al. 2011) provides images in 5 narrow and medium bands at violet and near ultraviolet wavelengths between roughly 200 and 400 nm. The wavelengths sampled by SuFI are: 214 nm at 10 nm bandwidth, 300 nm at 5 nm bandwidth, 312 nm at 1.2 nm bandwidth, 388 nm at 0.8 nm bandwidth and 396.8 nm (core of Ca II H) at 0.18 nm bandwidth. A 2048 × 2048 UV-enhanced CCD is employed, with a plate scale of 0.″02 per pixel. The highest cadence that can be achieved is an image every 2 s (if only a single wavelength is observed). In order to overcome aberrations caused by thermo-elastic deformations of the main mirror during flight, a phase-diversity technique (e.g. Paxman et al. 1992) is employed, also by the other science instrument, IMaX. For SuFI this implies an effective field of view of 15″ × 40″.

The Imaging Magnetograph eXperiment (IMaX; see Martínez Pillet et al. 2011) operates in the Zeeman $g = 3$ Fe I 525.02 nm line. Images in polarized light covering 50″ × 50″ are recorded at a spectral resolution of 85 mÅ, normally at 4 wavelengths within the spectral line and 1 in the nearby continuum. The full Stokes vector in these 5 wavelengths at a noise level of 10^{-3} is obtained in 30 s, which is the typical cadence for

most of the observations. A dual-beam approach is taken, with 2 synchronized 1k×1k CCD cameras.

The number of wavelength points (between 3 and 12) and of polarization states can be varied to obtain a higher cadence, or a better rendering of the line profile shape. The spectral resolution and sampling are achieved by using a thermally stabilized tunable solid-state Fabry-Pérot etalon in double pass together with a narrowband prefilter with a full width at half maximum of 0.1 nm.

The Image Stabilization and Light Distribution unit (ISLiD; see Gandorfer et al. 2011) allows simultaneous observations with the two science instruments by distributing the radiation according to wavelength (200–400 nm to SuFI; 525 nm to IMaX; 500 nm to CWS). It also houses a rapid tip-tilt mirror controlled by the CWS (see below).

The Correlating Wavefront Sensor (CWS; see Berkefeld et al. 2011) is of Shack-Hartmann type and is used in two ways, as a fast correlation tracker to derive control signals for a fast tip-tilt mirror, and as a slow wavefront sensor for active alignment control of the telescope secondary mirror.

The SUNRISE gondola (see Barthol et al. 2011) provides the housing for the telescope, instruments, power supply, etc. In addition, it is responsible for the precision pointing of the telescope towards the Sun. Finally, it is responsible for protecting the telescope, instruments, and subsystems from damage during landing (via parachute).

SUNRISE was flown on a zero-pressure stratospheric long-duration balloon launched on June 8, 2009 from ESRANGE near Kiruna in northern Sweden. It then floated westwards at a mean cruise altitude of 36 km and landed on Somerset island (northern Canada), suspended on a parachute, on June 13, 2009. At float altitude, virtually seeing-free observations were possible all the time (since the payload was above more than 99% of the Earth's atmosphere). Also, the balloon stayed above most of the ozone in the Earth's atmosphere, allowing high-resolution imaging in the UV at 214, 300, and 312 nm.

The loss of high-speed telemetry relatively soon after reaching float altitude (due to the failure of a rented commercial telemetry system), meant that no full images could be downloaded during the entire mission. Consequently, instrument commissioning and operations had to be carried out practically blindly. Nonetheless, the achieved spatial resolution was sufficiently high to resolve both small-scale magnetic and convective features (Lagg et al. 2010; Khomenko et al. 2010).

3. First Results

The Sun was extremely quiet during the entire flight of SUNRISE, so that almost all of the gathered data correspond to internetwork regions with occasional network elements. An overview of the data and first results is given by Solanki et al. (2010).

Images of the quiet Sun at disk centre in all 5 SuFI wavelengths are shown in Fig. 1a, whose grey scale is saturated at $\langle I \rangle \pm 3\sigma$ for each wavelength in order to allow a better intercomparison of the granulation, at the cost of overexposing the bright points. The brightness scale (see the gray-scale bars above the individual frames) already indicates the large rms contrasts of the imaged granulation, which reach up to 32% at 214 nm (cf. Hirzberger et al. 2010, for a complete study of the rms contrasts). At a number of the observed wavelengths the contrasts can be compared with those resulting from the 3D radiation-MHD simulations of Vögler et al. (2005) and are found

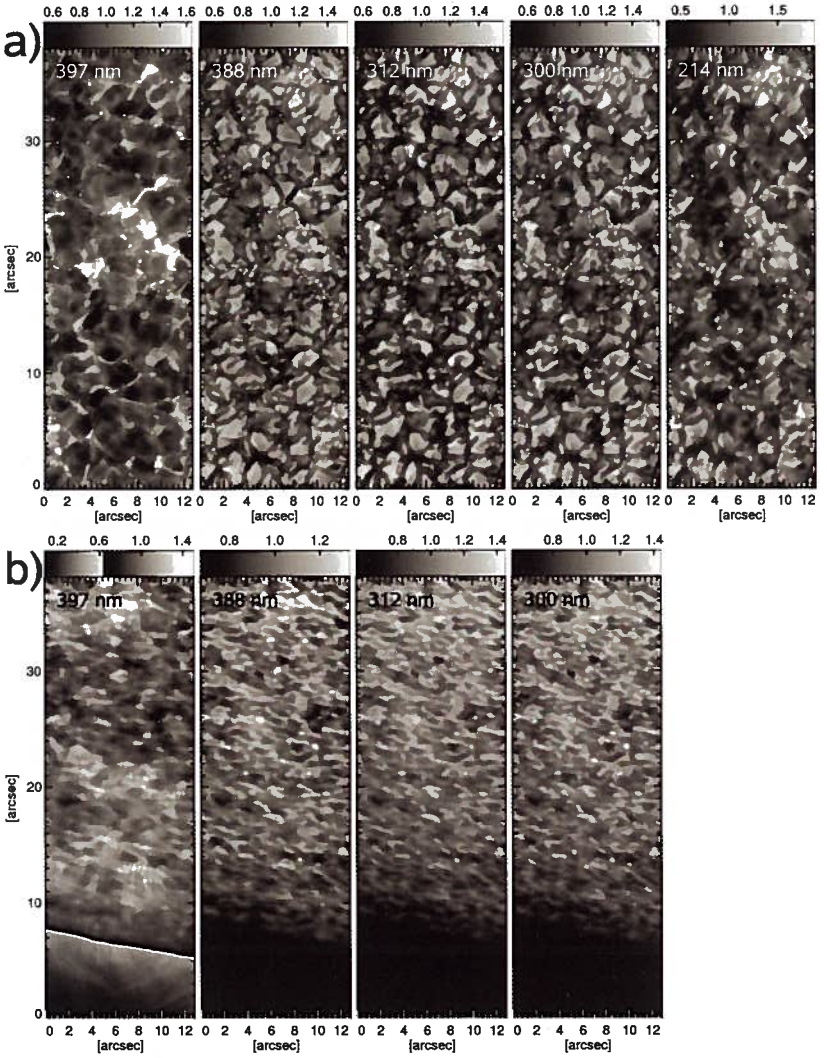

Figure 1. (*a*) Images of a patch of quiet Sun near disk centre recorded by the SuFI instrument in wavelength bands centred on 397, 388, 312, 300, and 214 nm (*from left to right*). The grey scale has been individually set to cover 3 times the rms range of each image. (*b*) Same as panel a, but at the solar limb. The Ca II H image (397 nm) is plotted with an enhanced brightness scale for the off-limb parts. No 214 nm data are available at this position.

to be in good agreement. This supports both the high resolution and very low stray light of SUNRISE SuFI data.

Bright points are prominent at all wavelengths sampled by SuFI, but are particularly so at 214 nm (they are 2.3 times as bright as the background at this wavelength, see Riethmüller et al. 2010), making them brighter than at any other wavelength studied so far.

Images at 4 SuFI wavelengths at the solar limb, in the general vicinity of the south solar pole are shown in Figure 1b. Obviously the structures at the south limb, although reminiscent of granules, are considerably smaller than those further away from the limb, in qualitative agreement with earlier results (Sánchez Cuberes et al. 2003). This smaller size could be related to greater prominence of granular sub-structure at the limb. In addition, polar faculae are visible, e.g. around $y = 13$, 20, and 36. Fibrils can be seen emanating from the faculae at $y \approx 13$ and spicules are clearly present off the solar limb (they became visible after the off-limb brightness was enhanced). Some of the spicule-like structures appear strongly inclined to the vertical and even slightly bent, so that they may actually be parts of quiet-Sun loops.

Figure 2 shows a snapshot of IMaX data products. Stokes V movies (see Solanki et al. 2010) reveal how dynamic the quiet Sun magnetic field is, with the weaker magnetic features, i.e., those in the internetwork, being particularly dynamic.

An investigation of the properties of small concentrations of strong magnetic fields in the quiet Sun showed that these have finally been resolved by IMaX on SUNRISE (Lagg et al. 2010). An inversion technique applied to retrieve the temperature stratification and the field strength could reproduce the observations well with a one-component, fully-magnetized atmosphere with a field strength exceeding 1 kG and a significantly enhanced temperature in the mid to upper photosphere compared to its surroundings, as illustrated in Figure 3. There three patches with kG field strengths are visible in the top frame. In the two middle frames the temperature at two different optical depths are plotted. Close to the continuum forming layer (2nd frame from top) the thermal map is dominated by granulation, while in the middle-photosphere (3rd frame) the magnetic elements stand out as the hottest features. This is consistent with semi-empirical flux-tube models describing magnetic elements. Consequently, it can be concluded that the SUNRISE measurements resolve the observed quiet Sun flux tubes. This result suggests that the SUNRISE data will allow further properties of these basic building blocks of the photospheric magnetic field to be determined rather directly.

SUNRISE observations show that the occurrence rate of patches of significant linear polarization signal (sensitive to the transverse component of photospheric magnetic field) is 1-2 orders of magnitude larger than values reported by previous studies (Danilovic et al. 2010). These features appear preferentially at granule boundaries with most of them being caught in downflow lanes at some point in their evolution. Only a small percentage are entirely and constantly embedded in upflows (16%) or downflows (8%). For the latter, the usual interpretation in terms of magnetic flux emerging from below cannot hold, so that they may be pointing to another source of horizontal magnetic flux.

Borrero et al. (2010) discovered that some of the patches of horizontal magnetic field in the internetwork are associated with supersonic upflows of magnetized gas. An interpretation in terms of localized jets and heating due to magnetic reconnection in photospheric layers between the emerging and previously present magnetic flux seems plausible.

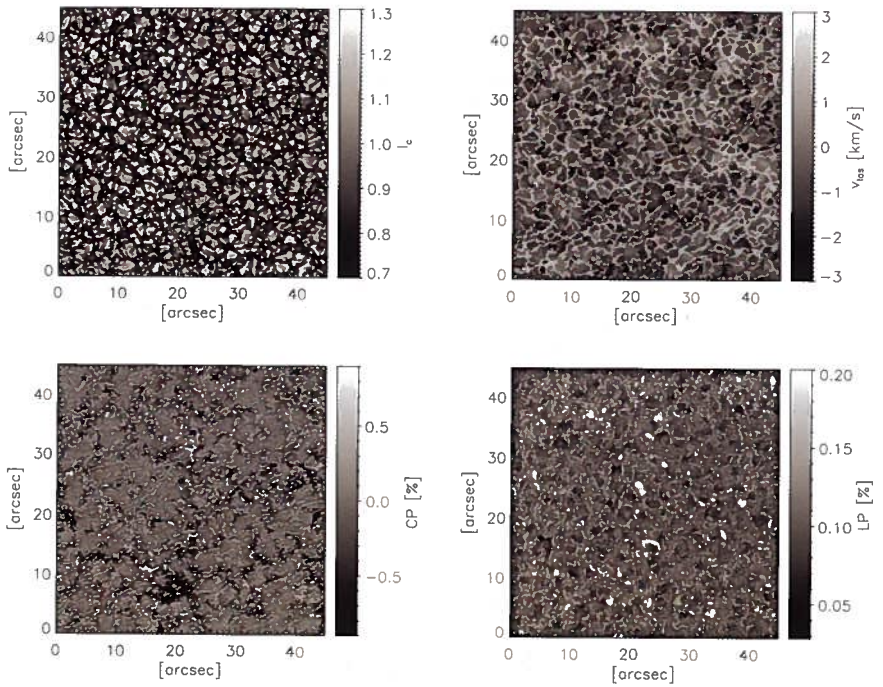

Figure 2. IMaX data. *Clockwise from upper left:* continuum intensity at 525.04 nm, line-of-sight velocity, net linear polarization averaged over the line (LP), and line-averaged Stokes V obtained from Fe I 525.02 nm (CP). All images are based on phase-diversity reconstructed data except for the linear polarization image (reconstruction increases the noise, so that a number of significant LP patches in the unreconstructed image are no longer sufficiently above the noise in the reconstructed data).

An analysis by Bello González et al. (2010) of high-resolution spectropolarimetric data obtained by IMaX on SUNRISE provides a total energy flux of approximately 6400–7700 W m^{-2} at a height of 250 km carried by waves with a period shorter than 3 min. This is more than twice the energy flux found in any previous work and lies within a factor of 2 of the energy flux needed to balance radiative losses from the chromosphere according to Anderson & Athay (1989). This result revives interest in acoustic waves for transporting energy to the chromosphere. An interesting conclusion is that the "missing" acoustic flux is hidden mainly at small spatial scales and not so much at high frequencies, where it has been assumed to lie in the past.

SUNRISE data have revealed vortical motion at small scales, with vorticity in both the horizontal and the vertical directions. Flows with vorticity in the vertical direction are seen by following small magnetic field patches (Bonet et al. 2010), while (smaller) horizontally directed vortex tubes have been discovered at the edges of granules by comparing time series of continuum images with 3D hydrodynamic simulations (Steiner et al. 2010).

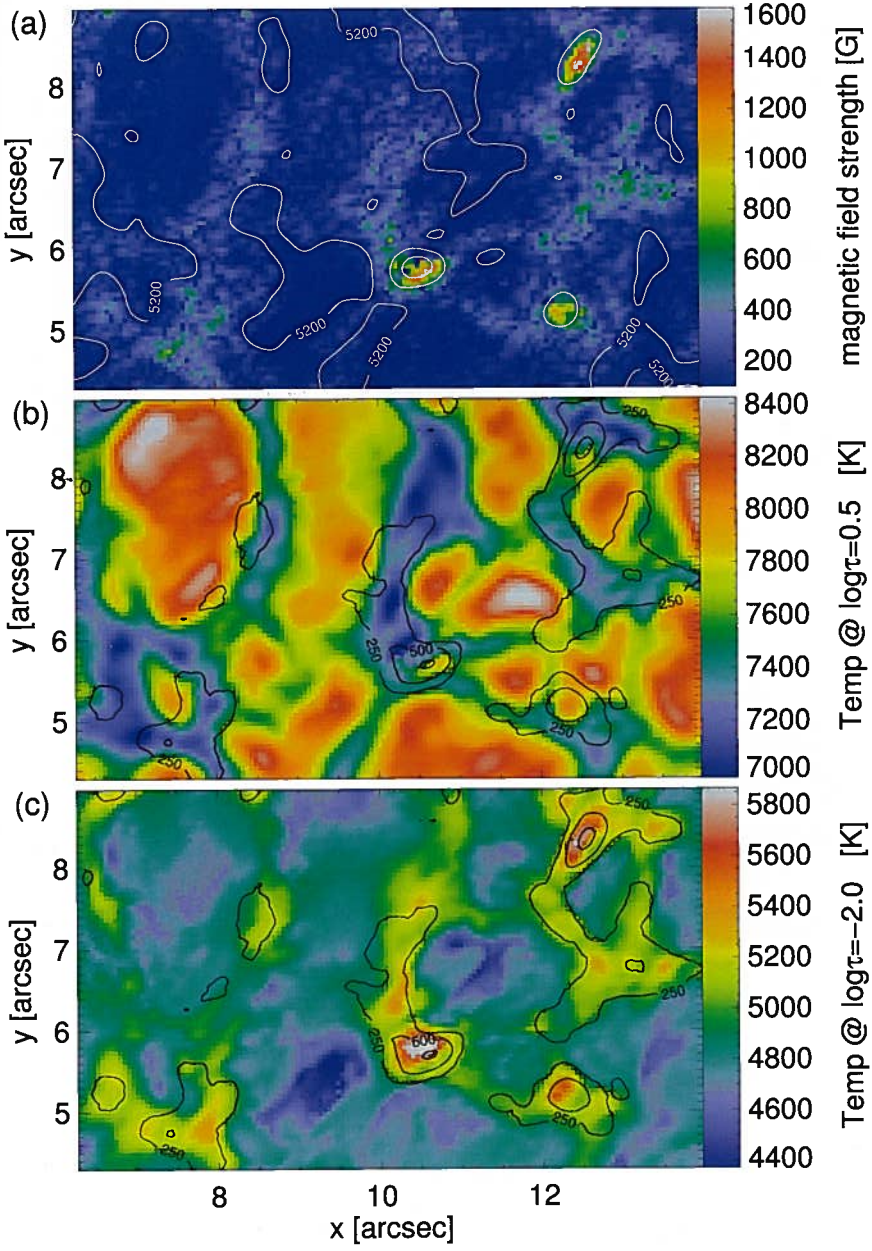

Figure 3. Maps of magnetic field strength (*panel a*) and temperature at two different optical depths (*panels b and c*). The contour lines of the magnetic field map (panel a) show the temperature at a continuum optical depth of 0.1 (5200, 5500, and 5800 K), the contour lines in panels b and c show the height-independent magnetic field strength (250, 500, and 1000 G).

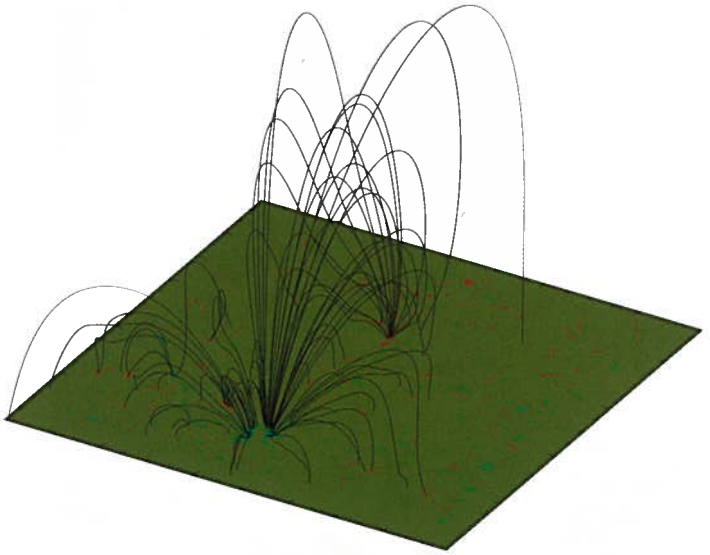

Figure 4. Magnetic loops computed with the help of a potential field model. Field lines have been integrated from photospheric pixels with a strength of above 300 G. Shown are a random selection of 10% of these magnetic loops.

The high resolution of the data is also indicated by the work of Khomenko et al. (2010), who show that the intergranular lanes, associated with broadened spectral lines, are bordered by narrow stripes of narrow spectral lines. These stripes, visible only at the high resolution achieved by SUNRISE, are located where the granular flows bend from up- to downflows, as comparisons with 3D hydrodynamic simulations show.

High degree p-modes are studied by Roth et al. (2010), who find that the power in waves with degree $l > 1000$ is enhanced over granules shortly before these start to split or explode, suggesting a connection between granule evolution and excitation of p-modes.

The magnetic field measured by SUNRISE in the photosphere has been extrapolated into the upper solar atmosphere by Wiegelmann et al. (2010). Figure 4 shows extrapolated field lines from a potential field model. The field line integration has been started at photospheric pixels with a field strength above the equipartition field strength of 300 G (these stronger field lines dominantly have one foot in a network patch). A statistical study of the connectivities of the extrapolated field shows that almost all of the magnetic field lines reaching the chromosphere or higher connect network with internetwork patches in the photosphere. Since the internetwork field is extremely dynamic and short-lived, this implies that the magnetic field in the upper atmosphere must also be changing very rapidly.

By local correlation tracking of intensity maps (Yelles Chaouche et al. 2011) determined that the internetwork fields are dominantly concentrated at the boundaries of mesogranular cells (approximately 85% of pixels with magnetic field greater than 100 G

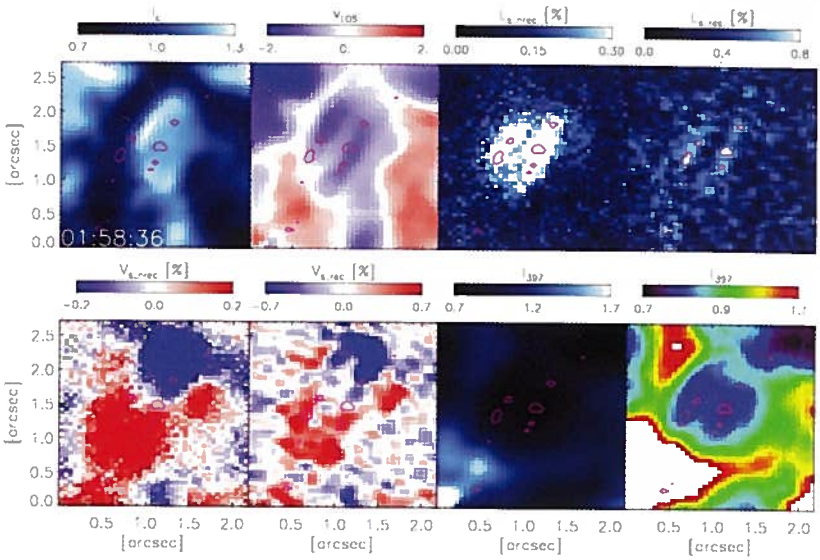

Figure 5. A snapshot of a small-scale bipole at approximately 3 min after the beginning of emergence. From *top to bottom* and *left to right*: continuum intensity, LOS velocity, the mean non-reconstructed and reconstructed linear polarization, the mean non-reconstructed and reconstructed circular polarization signal and filtergram centered at 397 nm (Ca II H). The bottom right panel shows the same Ca filtergram with saturated color scale. Pink contours outline the reconstructed linear polarization signal at 2 times the noise level.

are located there). The obtained mesogranular network harbors no preferred scales (i.e. no typical sizes of mesogranules), but rather a smooth distribution of scales between 1 and 10 Mm. This indicates that mesogranulation is not an intrinsic convective scale, thus contributing to the ongoing debate on whether there is a continuum of sizes for convection cells on scales above the granular one (e.g, Nordlund et al. 2009; Matloch et al. 2009, 2010).

Besides these first results that have already been published, further work is ongoing and additional results are emerging. A few examples are briefly described below.

The emergence of a small-scale bipole was followed by Danilovic et al. (2011), who found that the high resolution of the SUNRISE data allows magnetic substructure to be resolved in this emerging feature and shows that its rise is driven by buoyancy rather than just being carried by surrounding upflows. In this case, the field appears to be emerging in the form of two disjoint loops with upward velocity of approximately 1.2 km s^{-1} associated with the linear polarization signals. Figure 5 shows the event some 3 min after the appearance of a small linear polarization patch.

In this phase, the two slightly darker elongated regions separated by a slightly brighter ridge appear in SuFI Ca II H filtergrams, cospatially with two loops. Furthermore, the temperature profiles obtained from inversions confirm that these regions are cooler than the rest of the reversed granulation cell. Thus, the observations provide evidence that the reverse granulation gets disturbed by the presence of a rising magnetic flux tube, as demonstrated by the MHD simulations performed by Martínez-Sykora et al. (2008).

The discovery of oscillations of the magnetic field strength of internetwork features is reported by Martínez González et al. (2011). Thanks to the constant high spatial resolution of SUNRISE data these authors are able to determine the periodic change in the area covered by a given, fixed amount of magnetic flux. This corresponds to an oscillation in the magnetic field strength.

The dynamics of small-scale quiet-Sun brightenings seen in the Ca II H line core are being studied by Jafarzadeh et al. (in preparation). It is found that these brightenings are closely associated with photospheric magnetic flux, although they do not always completely overlap (with the overlap changing with time), suggesting that either the brightening is located at the side of the magnetic field, or the field displays a time-dependent inclination.

The above examples have been listed to demonstrate the wide variety of results that have been or are being deduced from SUNRISE data. These data are extremely rich, so that many more results are to be expected.

4. Conclusion

The SUNRISE observatory has provided high-quality, high-resolution images, Dopplergrams, and vector magnetograms at different positions on the solar disk. The extremely low solar activity level at the time of the science flight of SUNRISE means that these data mainly enable new insights into the quiet Sun.

An initial analysis of these data has already led to new insights into the magnetism, convection, oscillations, and waves in the quiet Sun. Given the richness and quality of the data and the fact that so far only a small fraction of them have been analyzed, we expect many more exciting results to follow. A reflight of SUNRISE during a period of higher solar activity is planned.

Acknowledgments. The German contribution to SUNRISE is funded by the Bundesministerium für Wirtschaft und Technologie through Deutsches Zentrum für Luft- und Raumfahrt e.V. (DLR), Grant No. 50 OU 0401, and by the Innovationsfond of the President of the Max Planck Society (MPG). The Spanish contribution has been funded by the Spanish MICINN under projects ESP2006-13030-C06 and AYA2009-14105-C06 (including European FEDER funds). The HAO contribution was partly funded through NASA grant number NNX08AH38G. This work has been partially supported by the WCU grant No. R31-10016 funded by the Korean Ministry of Education, Science and Technology.

References

Anderson, L. S., & Athay, R. G. 1989, ApJ, 336, 1089

Barthol, P., Gandorfer, A., Solanki, S. K., Schüssler, M., Chares, B., Curdt, W., Deutsch, W., Feller, A., Germerott, D., Grauf, B., Heerlein, K., Hirzberger, J., Kolleck, M., Meller, R., Müller, R., Riethmüller, T. L., Tomasch, G., Knölker, M., Lites, B. W., Card, G., Elmore, D., Fox, J., Lecinski, A., Nelson, P., Summers, R., Watt, A., Martínez Pillet, V., Bonet, J. A., Schmidt, W., Berkefeld, T., Title, A. M., Domingo, V., Gasent Blesa, J. L., Del Toro Iniesta, J. C., López Jiménez, A., Álvarez-Herrero, A., Sabau-Graziati, L., Widani, C., Haberler, P., Härtel, K., Kampf, D., Levin, T., Pérez Grande, I., Sanz-Andrés, A., & Schmidt, E. 2011, Solar Phys., 268, 1

Bello González, N., Franz, M., Martínez Pillet, V., Bonet, J. A., Solanki, S. K., del Toro Iniesta, J. C., Schmidt, W., Gandorfer, A., Domingo, V., Barthol, P., Berkefeld, T., & Knölker, M. 2010, ApJ, 723, L134

Berkefeld, T., Schmidt, W., Soltau, D., Bell, A., Doerr, H. P., Feger, B., Friedlein, R., Gerber, K., Heidecke, F., Kentischer, T., v. D. Lühe, O., Sigwarth, M., Wälde, E., Barthol, P., Deutsch, W., Gandorfer, A., Germerott, D., Grauf, B., Meller, R., Álvarez-Herrero, A., Knölker, M., Martínez Pillet, V., Solanki, S. K., & Title, A. M. 2011, Solar Phys., 268, 103

Bonet, J. A., Márquez, I., Sánchez Almeida, J., Palacios, J., Martínez Pillet, V., Solanki, S. K., del Toro Iniesta, J. C., Domingo, V., Berkefeld, T., Schmidt, W., Gandorfer, A., Barthol, P., & Knölker, M. 2010, ApJ, 723, L139

Borrero, J. M., Martínez-Pillet, V., Schlichenmaier, R., Solanki, S. K., Bonet, J. A., del Toro Iniesta, J. C., Schmidt, W., Barthol, P., Gandorfer, A., Domingo, V., & Knölker, M. 2010, ApJ, 723, L144

Danilovic, S., Beeck, B., Pietarila, A., Schüssler, M., Solanki, S. K., Martínez Pillet, V., Bonet, J. A., del Toro Iniesta, J. C., Domingo, V., Barthol, P., Berkefeld, T., Gandorfer, A., Knölker, M., Schmidt, W., & Title, A. M. 2010, ApJ, 723, L149

Danilovic, S., Pietarila, A., Riethmüller, T., et al. 2011, A&A, submitted

Gandorfer, A., Grauf, B., Barthol, P., Riethmüller, T. L., Solanki, S. K., Chares, B., Deutsch, W., Ebert, S., Feller, A., Germerott, D., Heerlein, K., Heinrichs, J., Hirche, D., Hirzberger, J., Kolleck, M., Meller, R., Müller, R., Schäfer, R., Tomasch, G., Knölker, M., Martínez Pillet, V., Bonet, J. A., Schmidt, W., Berkefeld, T., Feger, B., Heidecke, F., Soltau, D., Tischenberg, A., Fischer, A., Title, A., Anwand, H., & Schmidt, E. 2011, Solar Phys., 268, 35

Hirzberger, J., Feller, A., Riethmüller, T. L., Schüssler, M., Borrero, J. M., Afram, N., Unruh, Y. C., Berdyugina, S. V., Gandorfer, A., Solanki, S. K., Barthol, P., Bonet, J. A., Martínez Pillet, V., Berkefeld, T., Knölker, M., Schmidt, W., & Title, A. M. 2010, ApJ, 723, L154

Khomenko, E., Martínez Pillet, V., Solanki, S. K., del Toro Iniesta, J. C., Gandorfer, A., Bonet, J. A., Domingo, V., Schmidt, W., Barthol, P., & Knölker, M. 2010, ApJ, 723, L159

Kosugi, T., Matsuzaki, K., Sakao, T., Shimizu, T., Sone, Y., Tachikawa, S., Hashimoto, T., Minesugi, K., Ohnishi, A., Yamada, T., Tsuneta, S., Hara, H., Ichimoto, K., Suematsu, Y., Shimojo, M., Watanabe, T., Shimada, S., Davis, J. M., Hill, L. D., Owens, J. K., Title, A. M., Culhane, J. L., Harra, L. K., Doschek, G. A., & Golub, L. 2007, Solar Phys., 243, 3

Lagg, A., Solanki, S. K., Riethmüller, T. L., Martínez Pillet, V., Schüssler, M., Hirzberger, J., Feller, A., Borrero, J. M., Schmidt, W., del Toro Iniesta, J. C., Bonet, J. A., Barthol, P., Berkefeld, T., Domingo, V., Gandorfer, A., Knölker, M., & Title, A. M. 2010, ApJ, 723, L164

Martínez González, M. J., Asensio Ramos, A., Manso Sainz, R., Khomenko, E., Martínez Pillet, V., Solanki, S. K., López Ariste, A., Schmidt, W., Barthol, P., & Gandorfer, A. 2011, ApJ, 730, L37

Martínez Pillet, V., Del Toro Iniesta, J. C., Álvarez-Herrero, A., Domingo, V., Bonet, J. A., González Fernández, L., López Jiménez, A., Pastor, C., Gasent Blesa, J. L., Mellado, P., Piqueras, J., Aparicio, B., Balaguer, M., Ballesteros, E., Belenguer, T., Bellot Rubio, L. R., Berkefeld, T., Collados, M., Deutsch, W., Feller, A., Girela, F., Grauf, B., Heredero, R. L., Herranz, M., Jerónimo, J. M., Laguna, H., Meller, R., Menéndez, M., Morales, R., Orozco Suárez, D., Ramos, G., Reina, M., Ramos, J. L., Rodríguez, P., Sánchez, A., Uribe-Patarroyo, N., Barthol, P., Gandorfer, A., Knölker, M., Schmidt, W., Solanki, S. K., & Vargas Domínguez, S. 2011, Solar Phys., 268, 57

Martínez-Sykora, J., Hansteen, V., & Carlsson, M. 2008, ApJ, 679, 871

Matloch, L., Cameron, R., Schmitt, D., & Schüssler, M. 2009, A&A, 504, 1041

Matloch, Ł., Cameron, R., Shelyag, S., Schmitt, D., & Schüssler, M. 2010, A&A, 519, A52

Nordlund, Å., Stein, R. F., & Asplund, M. 2009, Living Reviews in Solar Physics, 6, 2

Paxman, R. G., Schulz, T. J., & Fienup, J. R. 1992, Journal of the Optical Society of America A, 9, 1072

Riethmüller, T. L., Solanki, S. K., Martínez Pillet, V., Hirzberger, J., Feller, A., Bonet, J. A., Bello González, N., Franz, M., Schüssler, M., Barthol, P., Berkefeld, T., del Toro Iniesta, J. C., Domingo, V., Gandorfer, A., Knölker, M., & Schmidt, W. 2010, ApJ, 723, L169

Roth, M., Franz, M., Bello González, N., Martínez Pillet, V., Bonet, J. A., Gandorfer, A., Barthol, P., Solanki, S. K., Berkefeld, T., Schmidt, W., del Toro Iniesta, J. C., Domingo, V., & Knölker, M. 2010, ApJ, 723, L175

Sánchez Cuberes, M., Vázquez, M., Bonet, J. A., & Sobotka, M. 2003, A&A, 397, 1075

Solanki, S. K., Barthol, P., Danilovic, S., Feller, A., Gandorfer, A., Hirzberger, J., Riethmüller, T. L., Schüssler, M., Bonet, J. A., Martínez Pillet, V., del Toro Iniesta, J. C., Domingo, V., Palacios, J., Knölker, M., Bello González, N., Berkefeld, T., Franz, M., Schmidt, W., & Title, A. M. 2010, ApJ, 723, L127

Steiner, O., Franz, M., Bello González, N., Nutto, C., Rezaei, R., Martínez Pillet, V., Bonet Navarro, J. A., del Toro Iniesta, J. C., Domingo, V., Solanki, S. K., Knölker, M., Schmidt, W., Barthol, P., & Gandorfer, A. 2010, ApJ, 723, L180

Tsuneta, S., Ichimoto, K., Katsukawa, Y., Nagata, S., Otsubo, M., Shimizu, T., Suematsu, Y., Nakagiri, M., Noguchi, M., Tarbell, T., Title, A., Shine, R., Rosenberg, W., Hoffmann, C., Jurcevich, B., Kushner, G., Levay, M., Lites, B., Elmore, D., Matsushita, T., Kawaguchi, N., Saito, H., Mikami, I., Hill, L. D., & Owens, J. K. 2008, Solar Phys., 249, 167

Vögler, A., Shelyag, S., Schüssler, M., Cattaneo, F., Emonet, T., & Linde, T. 2005, A&A, 429, 335

Wiegelmann, T., Solanki, S. K., Borrero, J. M., Martínez Pillet, V., del Toro Iniesta, J. C., Domingo, V., Bonet, J. A., Barthol, P., Gandorfer, A., Knölker, M., Schmidt, W., & Title, A. M. 2010, ApJ, 723, L185

Yelles Chaouche, L., Moreno-Insertis, F., Martínez Pillet, V., Wiegelmann, T., Bonet, J. A., Knölker, M., Bellot Rubio, L. R., del Toro Iniesta, J. C., Barthol, P., Gandorfer, A., Schmidt, W., & Solanki, S. K. 2011, ApJ, 727, L30